CHAPTER 1

Introduction and Literature Review

Contents

CHAPTER 1

Introduction and Literature Review

1.1 Introduction

The ultraviolet (UV) radiation has been the subject of interest for the survival and development of human kind since its invention by Johann Ritter in 1801. Although, it consists of less than 10% of the solar radiation (Internet Resource, IR1), but moderate skin exposure to natural solar radiation or artificial UV radiation helps in the synthesis of Vitamin D, killing germs, treating or preventing rickets, etc. On the other hand, excessive UV radiation to human body may lead to cataracts, sunburn and skin cancer, and even may also lead to the acceleration of the aging process. Besides the living beings, the output of crops and the lifespan of buildings are also strongly affected by the UV part of the solar radiation (Chen *et al.*, 2015). Fortunately, such diseases in the human beings are prevented by the absorption of most of the UV radiation from the sun at the stratospheric ozone layer. However, a steady lowering of about 4% in the total amount of ozone in Earth's atmosphere (the ozone layer), and a much larger springtime decrease in stratospheric ozone around Earth's polar regions (known as ozone hole) are the alarming threats to the increase in skin cancer in recent times. It is reported that a decline of 1% in the volume of the ozone layer may lead to an increase of 2% in UV radiation at ground level, which in turn, may lead to an increase of 3% in the incident rate of skin cancer (SE and SQ, 2014), and (Chen *et al.*, 2015). Thus, the study of UV photodetection has drawn considerable attention of the scientists for monitoring the

stratospheric ozone layer due to the growing effect of the UV radiation on the human life. Besides the ozone detection, UV photodetectors have also been the subject of research during last few decades for their potential applications in advanced communications, flame detection, air purification, and leak detections (Chen *et al.*, 2015).

The UV photodetectors are the semiconductor devices used to convert the incident UV radiation on the device into an electrical signal, either in the form of current or voltage, by following the Einstein's theory of photoelectric effect by *photon* radiation on metals. In 1900, Max Planck proposed that the energy is radiated in discrete small packets called quanta which were officially coined as "*photons*" by Frithiof Wolfers and Gilbert N. Lewis in 1926 (Kragh, 2014). The photoelectric effect phenomenon represents the emission of electrons from the surface of a metal due to the incidence of photons with energy larger than the work function of the concerned metal. The photoelectric effect is explored in the semiconductors to excite electrons from the valence band to conduction band by incident photons. The basic principle of working of the UV photodetectors consists of two parts: (i) the shifting of electrons from the valence band to conduction band of a semiconductor by incident photons of wavelengths in the UV region of the electromagnetic spectrum, and (ii) the collection of photo-excited conduction band electrons by an externally applied electric field. The relation between energy and wavelength of photons is given by $E = hc/\lambda$, where h is the Plank's constant, c is velocity of light and λ is the wavelength of the light. A photon of energy E is absorbed by an electron at the valence band for its shifting to the conduction band of a semiconductor with band gap energy E_g if $E \geq E_g$. Thus, the excitation of an

electron from the valence band to conduction band depends on the energy (*i.e.* wavelength) of the incident photons. Based on the wavelengths, the UV spectrum can be typically classified into three kinds namely UV A (315-400 nm), UV B (280-315 nm) and UV C (100- 280 nm) (Internet Resource, IR2) as shown in Figure 1. 1 The wavelength range of ~315 nm- 400 nm is called UV-A region while ~280 nm-320 nm is known as UV-B region and ~100 nm -280 nm is designated as UV-C region (Monroy *et al.*, 2003). The wavelength ranging from 220 nm to 280 nm, called the deep UV region, lies in the solar-blind region while the UV region below 180 nm wavelengths is in the vacuum UV region. The UV-B and UV-C are the strongest and potentially most harmful UV regions in the electromagnetic spectrum (Chen *et al.*, 2015).

With the constant improvement in the nanofabrication techniques, the fabrication of semiconductor nanostructures based photodetectors have gained a wide popularity in recent times. There are basically two categories of nanofabrication methods: top-down and bottom-up approaches (Chen *et al.*, 2015) and (Yang *et al.*, 2010). In the top-down approach, various thin film pattern based device structures are achieved by lithography or patterning techniques, such as focused ion beam (FIB), micro-electro-mechanical system (MEMS), Nanoimprint lithography (NIL), E-beam lithography (EBL) nanotechnology, among others (Chen *et al.*, 2015). On the other hand, the desired nanostructures, such as Nanocubes (Zhao *et al.*, 2014), Nanospheres (Xu *et al.*, 2015), quantum dots (Ick Son *et al.*, 2013), Nanobelts (Fang *et al.*, 2009) and solution based low-temperature Nano thin films (Wang *et al.*, 2014), (Kumar, Kumar, Rawat, *et al.*, 2017) are fabricated by individual atoms and molecules in the bottom-up methods. Various synthesis techniques such as the chemical vapor deposition (CVD), vapor–liquid–solid (VLS) /vapor–solid (VS) processes, hydrothermal /solvothermal reaction,

solution-based self-assembly, template-assisted growth and subsequent heat-treatment processes, etc. are used for fabricating various nanostructure based UV photodetectors (Chen *et al.*, 2015). The solution processed synthesis techniques are believed to be the simplest and most cost effective techniques for nanoelectron device fabrication. Although, GaN is the most widely used semiconductor for UV applications, however, various metal oxide nanustructure based UV detectors have drawn considerable attention due to their lower processing cost. In the present thesis, an attempt has been made to fabricate and characterize some ZnO colloidal quantum dots (CQDs) based visible blind spectrum selective UV detectors on silicon and low-cost glass substrates using low-cost solution processed fabrication methods. The spectrum selective photodetectors are the devices capable of detecting UV radiation over a narrow wavelength region in the electromagnetic spectrum. The spectrum selectivity is measured in term of the full-width at half-maxima (FWHM).

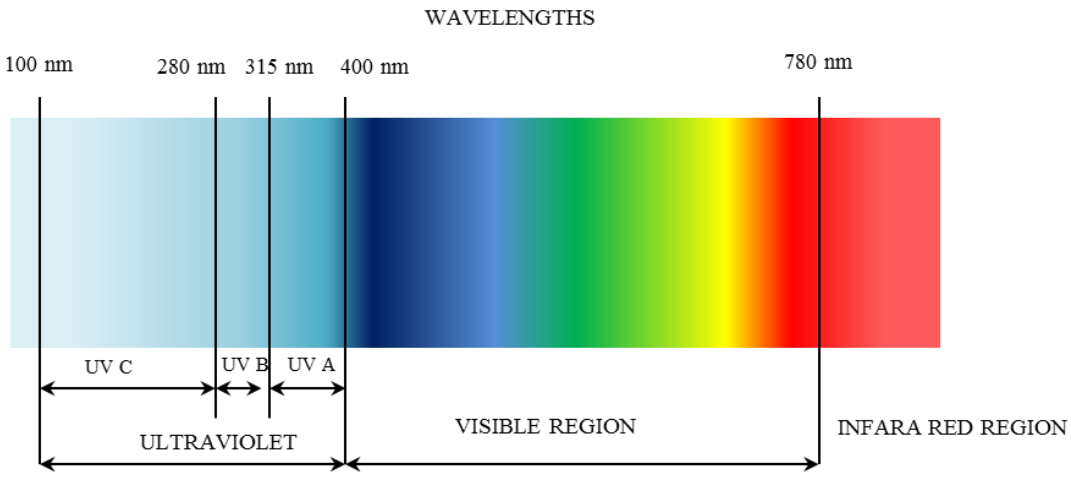

Figure 1. 1: Electromagnetic spectrum of the sunlight**.**

The performance of any photodetector can be evaluated from the current-voltage (I-V) characteristics under dark and illuminated conditions. Several performance parameters such as the quantum efficiency, spectral responsivity, spectral selectivity, noise, detectivity and time response characteristics are used to measure the performance of the detectors. In the present thesis, we have investigated for the I-V characteristics, responsivity, selectivity and time response characteristics of some ZnO CQDs based UV photodetectors using low-cost solution processed methods. Thus, we define the following important terms to be used in the present thesis.

- Responsivity (R_e): It is defined as the generated outcome (current or voltage) per incident optical power at a incident wavelength (λ). Therefore it has the unit usually expressed either in A/W or V/W.
- Quantum Efficiency (η): The quantum efficiency of a photodetector is defined as the ratio of the number of photogenerated carriers to the number of photons of a given energy incident on the detector. It may be given either as a function of wavelength or as energy.
- Spectral selectivity: It is defined as the ability of a photodetector to detect accurate and intended energy photons without any interference of the adjacent wavelengths. It is often expressed in term of the *full-width at half maxima* (FWHM) of the responsivity versus wavelength characteristics of a photodetector.

- FWHM: The FWHM is defined as the difference between the two extreme values of the wavelength at which the responsivity is equal to half of its maximum value.

- Time Response: The time response the photodetectors are expressed in terms of the rise time (t_r) and fall time (t_d) of the output signal when a pulsed light is incident on the detector (Smith and Honda, 1973). The rise time (t_r) is the measure of the time response of a photodiode to a stepped light input, and is defined as the time required for the output to change from 10 % to 90 % of the steady output level. Similarly, the fall time (t_d) is measured as the decay from the 90% to 10% of the falling edge of the output rectangular pulses of the detector when a pulsed source of light is incident on the detector.

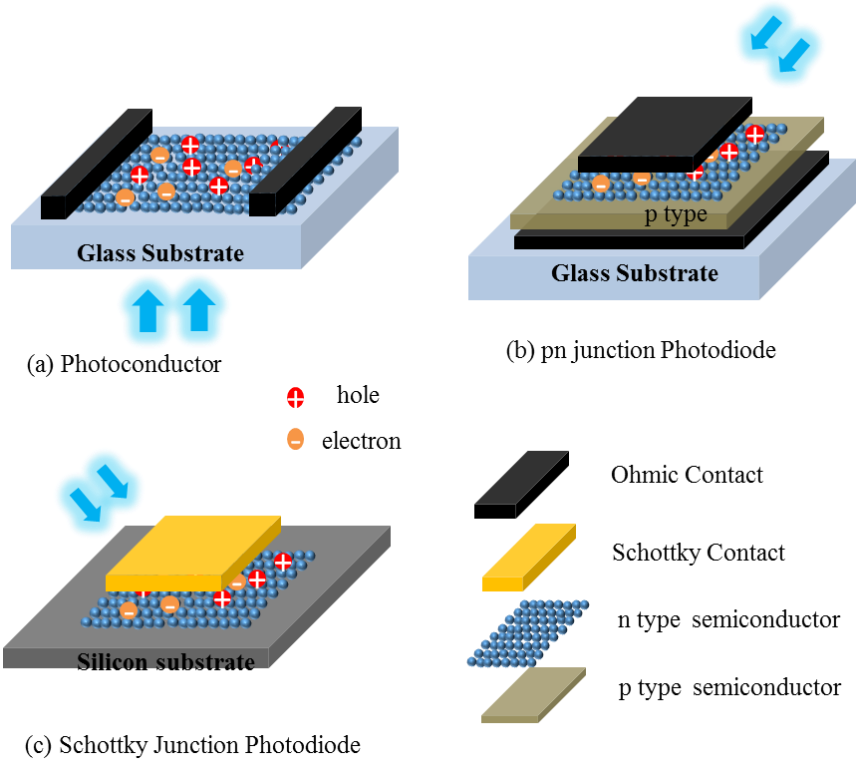

Figure 1. 2: Schematic structures of photoconductor and photodiode.

1.2 Photodetector Structures

The photodetection capability depends on the type of device structure and active semiconductor material used for the photodetector. A number of different photodetector structures such as photoconductor, photodiode, phototransistor, and photojunction field effect transistor have been reported (Monroy *et al.*, 2003). The most commonly used photodetector structures are photoconductors, pn junction photodiodes and Schottky junction photodiodes shown in Figure 1. 2 (a). They are briefly discussed as follows.

1.2.1 Photoconductors

Photoconductors, also called photoresistors or light dependent resistors, are the most basic form of two terminal photodetectors where the incident photons are used to create photo-excited electron-hole pairs to change the conductivity of a semiconductor by the photoelectric effect. The device structure consists of two Ohmic contacts placed on a semiconductor bar as shown in Figure 1. 2. When the photons of energy larger than the band gap energy of the active semiconductor, electrons are excited from the valence band to conduction band thereby creating holes in the valence band and free electrons in the conduction band due to photoelectric effect. The photogenerated electron-hole pairs reduces the conductivity (and hence the resistance) of the active semiconductor material. As a result, current flowing through the semiconductor bar increases with incident photon flux density for any fixed bias voltage applied between the two Ohmic electrodes as shown in Figure 1. 3. The change in the current density (J) due to the incidence of the photons can be represented as follows:

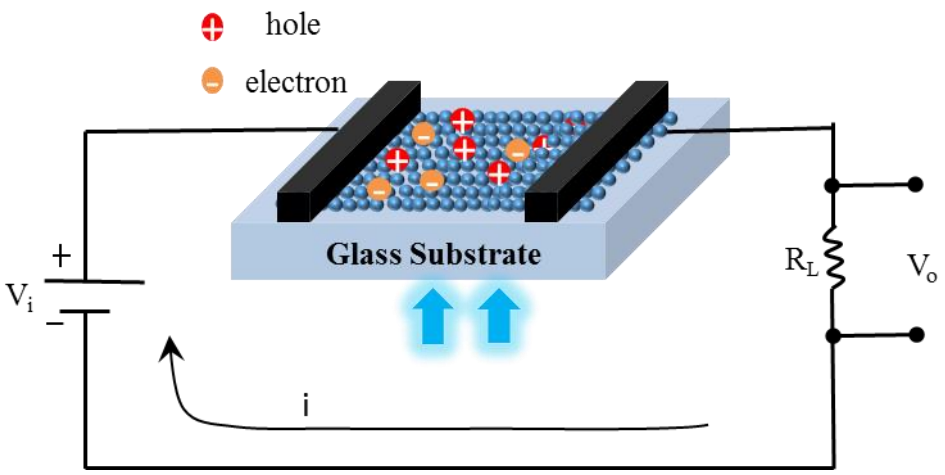

Figure 1. 3: Photoconductor working principle under UV illumination.

The total current density, J in the semiconductor can be described as

$$J = J_{dark} + J_{photo} \tag{1.1}$$

where J_{dark} is the dark current when no illumination is incident of the device and J_{photo} is the photocurrent due to excess photogenerated electron-hole pairs discussed earlier.

Now, assuming an n-type semiconductor in the device, J can be expressed in terms of the conductivity (σ) of the semiconductor and applied electric field ($\mathcal{E}$) as:

$$J = \sigma \varepsilon \tag{1.2}$$

$$\sigma = \rho \mu \tag{1.3}$$

where μ_e is the mobility of the electrons and ρ is the charge density defined as

$$\rho = n q \tag{1.4}$$

where n is carrier concentration and q is the electronic charge.

The incident photon flux density, say ϕ, increases equal electron (Δn) and hole (Δp) concentrations (i.e., $\Delta n = \Delta p$) due to photoexited carriers. Thus, J_{photo} due to ϕ can be defined as (Jin *et al.*, 2014)

$$J_{photo} = (\mu_e + \mu_h)\Delta n \, q\varepsilon \tag{1.5}$$

where μ_e and μ_h is the mobility of electrons and hole.

$$\Delta n = \frac{\eta \phi \tau}{WA} \tag{1.6}$$

where η is quantum efficiency, τ is excess carrier recombination time, W is channel length of photoconductor, and A is the active cross section area of photoconductor.

The photocurrent can be written as,

$$i_{photo} = J_{photo} A \tag{1.7}$$

Assuming $v_e = \mu_e \varepsilon,\ v_h = \mu_h \varepsilon,\ t_e = \frac{W}{v_e},$ and $t_h = \frac{W}{v_h}$ as the drift velocity of electron, drift velocity of hole, transit time of electron and transit time of hole, respectively, Eqn. (1.7) can be written

$$i_{photo} = \eta \phi \tau \, q\left(\frac{1}{t_e} + \frac{1}{t_h}\right) \tag{1.8}$$

Note that the photon flux density is the number of photons of wavelength λ given by

$$\phi = \frac{P_{opt}}{h\nu} = \frac{P_{opt}\lambda}{hc} \tag{1.9}$$

where, P_{opt} is the incident optical power density, h is plank constant, and v is frequency of the incident photon.

From Eq 1.8 and Eq. 1.9, we can define the photoresponsivity (R) as (Pal *et al.*, 2012)

$$R = \frac{i_{photo}}{P_{opt}} = \frac{\eta}{1240}\left(\frac{\tau}{t}\right)\lambda(\text{nm}) \tag{1.10}$$

where $t = \left(\frac{1}{t_e} + \frac{1}{t_h}\right)^{1/2}$.

Note that the factor of $\frac{\tau}{t}$ defines the gain of the photoconductor. The values of τ and t depend on the type of materials used for the fabrication of the photoconductor and the channel length (W) of the fabricated photoconductor.

1.2.2 Photodiodes

The photodiodes are also two terminal devices whose conduction mechanism is unidirectional to provide rectification. They are either the pn junction diodes or Schottky junction diodes using a wideband gap semiconductor (i.e. ZnO CQDs in the present thesis) as the active material for phtodetection of desired wavelengths. The flow of current and applied biasing define the operation of the both types of photodiodes. The biasing for which the photodiodes conduct is called forward bias while the complementary biasing is called reverse bias. The rectifying junction between a metal and a semiconductor used for photodetection is called Schottky junction photodiodes (Sze, 2002) while a pn homojunction (Lopatiuk-Tirpak *et al.*, 2007) or heterojunction diodes (Hazra and Jit, 2014) used for photodetection is called pn junction photodiodes.

In both the cases, a depletion region of width (W) is formed at the metallurgical junction which can be given as (Sze, 2002)

$$W = \sqrt{\frac{2 \in_s (V_{bi} - V)}{qN_d}} \tag{1.11}$$

where ϵ_s is the effective dielectric constant, N_d is the donor concentration, V_{bi} is the built-in potential developed across the depletion region at thermal equilibrium, and V is the externally applied potential to operate the photodiode.

Equation (1.11) is assumed for the Schottky junction or a one sided abrupt pn junction. Clearly, the width of the depletion region is a function of the applied external potential which is increased with the reverse bias voltage as evident from Eq. 1.11. The depleted region of the photodiodes play significant roles in determining the photocurrent of the device. When the light is incident on the devices, photogenerated electro-hole pairs generated in the depletion region. The generated electron-hole pairs are drifted out by the presence of electric field in that region thereby resulting in the photocurrent of the device. Since W is increased under the reverse bias condition, the photodiodes are normally operated under reverse bias condition for improving the photoresponse of the detectors. The photogenerated electrons are drifted towards n-region and holes are drifted towards p-region as shown in Figure 1. 4. The electrical circuit of the photodiodes is shown in Figure 1. 5. The properties of active semiconducting material in the detector defines the figure of merit of the photodetectors as discussed in case of photoconductors.

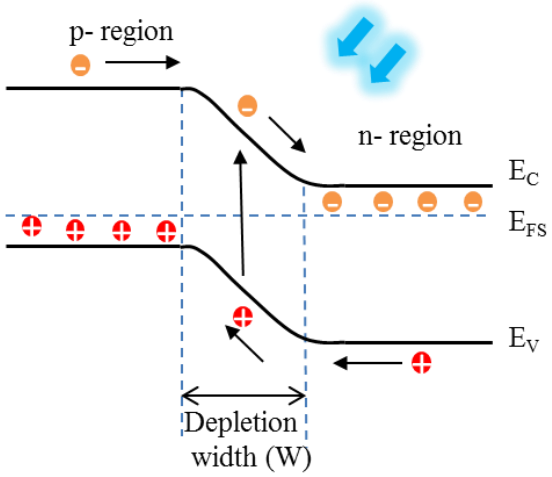

Figure 1. 4: Energy band diagram of pn junction.

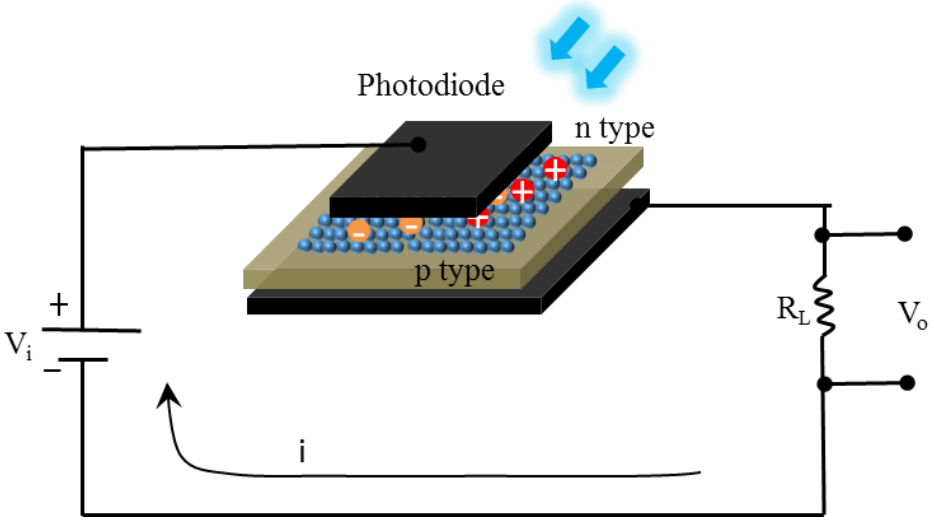

Figure 1. 5: Photodiode circuit schematic under UV illumination.

1.3 Semiconductor Materials for UV Photodetectors

The UV photodetectors (PDs) have attracted extensive attention owing to their broad application segment from civil to military domains including UV-photography, flame sensing, water sterilization, biomedical sensing and biological treatments (Monroy *et al.*, 2001), (Aufiero *et al.*, 2006). Wide varieties of UV PDs are used for the UV detection including the Si based photodetectors and photomultipliers. Silicon is the most abundant semiconductor material with an indirect band gap of 1.19 eV showing

the panchromatic absorption range from UV to near IR. Thus the Si based devices can be actively used for solar cells and PDs. However, for designing a Si based PD, we require a filter to stop the low energy photons and a photomultiplier to enhance the efficiency of the PDs (Liu *et al.*, 2010; Shi and Nihtianov, 2012). The involvement of the external filter (Bayer's filter) to achieve the UV photodetection out of the panchromatic absorption range of Si reduces the incident photon count on the active layer of the PD which greatly reduces the photoresponse of the PDs. The fabrication of external filter also increases the fabrication complexity thereby increasing cost of the Si based UV PDs. The above limitations of the Si based UV PDs can be overcome by using wide band gap materials such as Diamond, GaN, SiC, and transition metal oxides (TMOs) such as ZnO, TiO_2, and NiO. The optical absorption range of the TMOs is limited to the UV region only and hence are best suitable for the fabrication of low-cost solution processed UV PDs. Further, TMOs based UV PDs are also suitable for room-temperature operation. The thermal conductivity of the TMO based wide band gap materials are higher than that of Si (Monroy *et al.*, 2003) which make them suitable for high-temperature and high-power applications.

Among various metal oxide semiconductors, the ZnO is widely researched for UV photodetection due to the various attractive properties such as its direct band gap of 3.35 eV, higher exciton energy 60 meV, higher radiation hardness, and higher thermal and chemical stability (Somvanshi and Satyabrata Jit, 2014). The ZnO can be found in three different structures namely hexagonal wurtzite, zinc blend and cubic rock salt. Among them, the hexagonal wurtzite structure shown in Figure 1. 6 is stable for UV detection at room temperature and pressure. Some typical parameters values of the ZnO are listed in table 1.1.

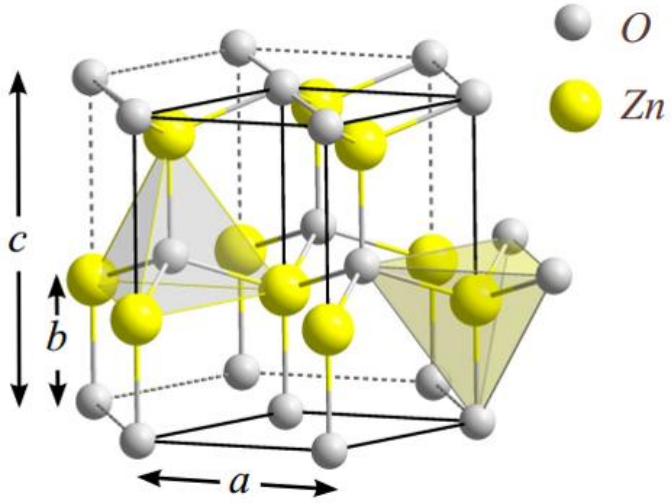

Figure 1. 6: Wurtzite crystal structure of ZnO with lattice parameters: a=3.250 Å, c=5.207Å (Internet Resource, IR3)

A number of ZnO nanostructure based UV photodetectors fabricated by various methods have been reported in the literature (Omnès *et al.*, 2007; Das *et al.*, 2010). The ZnO based photodetectors are fabricated via multiple routes such as RF sputtering (Al-Hardan *et al.*, 2011), Thermal deposition (Somvanshi and S. Jit, 2014), and solution processing (Yadav, Pandey, *et al.*, 2015). However, the solution based ZnO deposition technique is considered to be the simplest and most cost effective method for large area nanoelectronics (Tsay *et al.*, 2010). Several multifaceted ZnO based UV photodetector structures based Schottky Junction (Brillson and Lu, 2011), Metal-Semiconductor-Metal (D.-Y. Guo *et al.*, 2014), *p-n* junction (Liu *et al.*, 2010), and heterojunction (Hazra and Jit, 2014) have been reported in the literature.

Table 1. 1: Some typical properties of ZnO (Singh, 2011)

Parameters	**Values**
Energy gap	3.4 eV, direct bandgap
Density	5.606 g cm^{-3}
Crystal structures	Wurtzite, rock salt and zinc blend
Stable phase at 300K	Wurtzite
Melting point	1975 ºC
Lattice constants	a= 0.32495 nm, c= 0.52069 nm
Relative dielectric constant	8.66
Refractive index	2.0041
Intrinsic carrier concentration	1016 to 1020 cm^{-3}
Exciton binding energy	60 meV
Electron effective mass	0.24 m_0
Electron hall mobility at 300 K	200 cm^2 v^{-1} s^{-1}

1.4 Ssemiconductor Nanostructures for Photodetector Applications

The semiconductor nanostructures have drawn special interests for various sensing applications due to their larger surface-to-volume than their bulk counterparts. Further, the electronic and optical properties of the semiconductor nanostructures can be largely modified by varying their size, shape and assembling. The size of the nanostructures hugely modifies the electronic band structures due to a phenomenon called quantum confinement effect. The effect of quantum confinement comes into picture for the

particles with the size ranging in 1-10 nm (Klimov, 2010). The quantum confinement limits the natural separation length of electron-hole pairs (exciton) generated using incident photon flux. The natural separation between the electron-hole pair as exciton can be approximated as Bohr's radius (Klimov, 2010) defined as:

$$a_b = \in \frac{m}{m^*} a_0 \tag{1.12}$$

where m^* is the mass of the particle, m is the rest mass of the electron, and a_0 is the Bohr's radius of hydrogen atom.

The quantum carrier confinement in the semiconductor nanostructures can take place in any one or more directions depending on the size of the nanostructures. Depending on the dimension of nanostructures, they are classified into four kinds namely three dimensional (3-D), two dimensional (2-D), one dimensional (1-D) and zero dimensional (0-D) nanostructures (Jagadish and Pearton, 2006) and (Tiwari et al., 2012) which are briefly defined as follows:

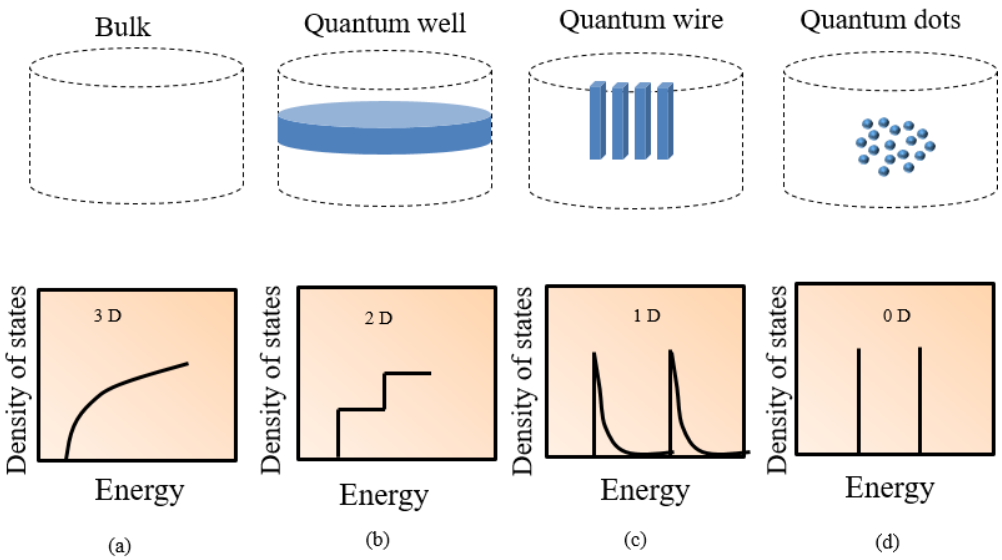

Figure 1. 7: Band structure of QDs and bulk semiconductor

1.4.1 Three Dimensional (3-D) Nanostructures

Three dimensional (3-D) nanostructures are basically the bulk materials with sizes beyond the nanoscale regime (i.e. 1-10 nm) in all the three dimensions and hence no quantum confinement of carriers take place in any of the three directions. In other words, carriers are free to move in all directions in the 3-D semiconductor nanostructures. The detailed schematic and the band diagram of the 3-D nanostructures are shown in Figure 1. 7 (a).

1.4.2 Two Dimensional (2-D) Nanostructures

When the sizes of the nanostructures are much beyond the nanoscale regime of 1-10 nm (i.e. >> 10 nm) while the size in the remaining one direction is in the nanoscale regime (i.e. <10 nm), they are called 2-D nanostructures. In this case excitons are confined only in one direction (which has dimension in the nanoscale regime) while they are free to move in other two directions. The confinement of the exciton in one direction is achieved by the small size of particle in that direction (1-10 nm) of the nanostructure. When the 2-D nanostructures provide a high potential barrier across one dimension so that the charge remains trapped in that dimension, they are called quantum well as shown in Figure 1. 7 (b). The size of the quantum well defines the energy levels of the electrons. Any change in the size of the quantum well modifies the energy levels of the electrons and subsequently modifies the band diagram also as shown in Figure 1. 7 (b). The modification in energy bands can be estimated via the effective-mass approximation model for the energy levels $(E_n (k_y k_z))$ inside the quantum well and the size of the quantum well (a_x) as given below (Arivazhagan, 2013):

$$E_n(k_y k_z) = \frac{n^2\pi^2\hbar^2}{2m^*(a_x^2)} + \frac{\hbar^2}{2m^*}(k_y^2 + k_z^2)$$

$$\psi = \phi(x)\exp(ik_y y + ik_z z) \quad (1.13)$$

where n, $\hbar$, k_y, k_z and a_x are the quantum number, Planck's constant divide by 2π, wave vectors in y and z direction and confinement dimension, respectively and Ψ denotes the electron wave function.

It is observed that the energy levels are inversely proportional to the square of the confinement dimension (a_x). Such modifications in energy bands of the 2-D semiconducting nanostructures are widely used in lasing action (Nakamura *et al.*, 1996), LEDs (Tran *et al.*, 1999), photodetectors (Gruber *et al.*, 2004) of quantum well lasers.

1.4.3 One Dimensional (1-D) Nanostructures

If one of the three dimensions of the nanostructures is much beyond the nanoscale regime (i.e.>> 10 nm) while other two are in the nanoscale regime (< 10nm), they are called one dimensional (1-D) nanostructures. In such nanostructures, the confinement of excitons take place in two directions except the one with dimension more than 10 nm. The most common type of structures are nanowire and nanaorods. The energy bands of the 1-D nanostructure can be modified by varying any of the two or both dimensions and hence Eq. 1.13 can be re-written as:

$$E_n(k_z) = \frac{\pi^2\hbar^2}{2m}\left(\frac{n_x^2}{a_x^2} + \frac{n_y^2}{a_y^2}\right) + \frac{\hbar^2}{2m^*}(k_z^2)$$

$$\psi = \phi(x)\,\phi(y)\exp\,(ik_z z) \quad (1.14)$$ where

the x and y directions are the confined directions and the exciton are free in z direction.

The 1-D nanostructures are widely used for photodetectors (Novotny *et al.*, 2008), LED (Pan *et al.*, 2013), and solar cells (Jia *et al.*, 2012).

1.4.4 Zero Dimensional (0-D) Nanostructures

The semiconductor nanostructures in which the excitons are confined in all the three directions are called zero-dimensional (0-D) nanostructures. Quantum dots (QDs) are the examples of 0-D nanostructures which lie in between the molecular region and bulk region. The quantum confinement effect is much more dominated in QDs as compared to 2-D and 1-D based nanostructures due to confinement of excitons in every direction of the material. The slightest change in the size of the QDs modifies the energy band of the semiconductor larger than that of the 2-D and 1-D based nanostructures. The allowable energy bands of the confined excitons in the QDs can be approximated via the potential function $V(r)$ of the particle-in-a-box as:

$$V(r) = \begin{cases} 0 & r < a \\ \infty & r > a \end{cases} \tag{1.15}$$

where "*a"* is the radius of potential well.

The Eq. 1.14 can be modified by using Eq. 1.15 as (Kumar, Kumar, Mukherjee, *et al.*, 2017):

$$E_n = \frac{\pi^2 \hbar^2}{2m}\left(\frac{n_x^2}{a_x^2} + \frac{n_y^2}{a_y^2} + \frac{n_z^2}{a_z^2}\right)$$
$$\psi = \phi(x)\,\phi(y)\,\phi(z) \tag{1.16}$$

where a_x, a_y and a_z are particle directions.

The solution provided above is valid for only single exciton. For the case of multiple exciton generation, there will be coulombic interaction (E_c) between the charge pairs which can be approximated as:

$$E_c = k_e q^2 \left(\frac{1}{b_x} + \frac{1}{b_y} + \frac{1}{b_z} \right) \tag{1.17}$$

where b is the natural separation of the electron hole pair in direction *x, y* and *z, and* k_e is electron transfer rate.

The modified Eq.1.16 can now be modified by taking the account of coulombic interaction as (Klimov, 2010).

$$E_n = \frac{\pi^2 \hbar^2}{2m} \left(\frac{n_x^2}{a_x^2} + \frac{n_y^2}{a_y^2} + \frac{n_z^2}{a_z^2} \right) - E_c, \tag{1.18}$$
$$\psi = \phi(x)\phi(y)\phi(z)$$

The reduction in the size of QDs leads to increase in the spacing between the energy bands. The quantum confinement effect converts the continuous bands of bulk semiconductor into discrete band structure in QDs as shown in Figure 1. 7 (d). The properties of the semiconductor nanostructures can be utilized to design various photodetectors with highly spectrum selective nature.

1.5 Spectrum Selective Photodetectors

Spectrum selective photodetectors are the class of detectors which are capable of detecting lights over a very narrow selected wavelengths. Such type of detectors have a narrow Gaussian pulse like responsivity versus wavelength characteristics. The spectrum selective photodetectors are used for multiple applications such as imaging

system, environmental surveillance, mimicking human eye, and artificial intelligence (Fang *et al.*, 2015). For imaging systems, the spectral response window of the photodetector should be a narrowband in nature (Jansen Van Vuuren *et al.*, 2010). In the state-of-the-art photodetectors, spectrum selectivity is achieved by using dichroic prism or a set of optical filters (Bayer, 1976). This approach increases the architectural complexity of the device. Further, the use of additional filters degrade the responsivity of the detector thereby restricting the higher pixel density in imaging systems by reducing the image sharpness (Park *et al.*, 2014). Further, the external filters are susceptible to cross-interference and cross-talks which can lead to serious side peaks and distortion in existing response (Baierl *et al.*, 2012) of the detectors. Another approach to achieve the spectrum selectivity is to use an increased absorption over a specified region by using plasmonic effects (An *et al.*, 2009) in the photoactive semiconducting material with a narrow absorption band in the desired spectrum of the detectors (Lin *et al.*, 2015). However, the use of plasmonic effects to achieve the narrowband UV detection is restricted by the limited availability of the metals showing plasmonic effects in UV region (McMahon *et al.*, 2013). Further, the metallic nanoparticles suitable for the plasmonic effect in UV region are suffered from the surface oxidation (Sanz *et al.*, 2013). Moreover, the photoactive materials with narrow absorption have very low photoresponse which reduces the figure of merit of photodetectors. Since the electronic and optoelectronic properties are highly dependent on the size of the quantum dots (QDS), we have explored the colloidal ZnO QDs for fabricating highly spectrum selective photodetectors with reasonable responsivity characteristics without using any filters in the present thesis.

1.6 Some State-Of-The-Art Works on ZnO Based UV Photodetectors

The ZnO based UV photodetector was reported as early as in 1940s (Mollow, 1954). However, the significant progress on the ZnO based photodetectors has been started since 1980 (Liu *et al.*, 2010). Various types of ZnO nanostructures have been explored for optimizing the performance of the ZnO based UV photodetectors during last several decades. However, since the major objective of the present thesis is to focus on the fabrication and characterization of some solution processed ZnO QDs based spectrum selective UV photodetectors, we will devote the present section to review some ZnO based UV photodetectors with emphasis on spectrum selective responsivity characteristics.

1.6.1 ZnO Quantum Well Based Devices

ZnO and ZnO based ternary compounds such as ZnMgO have been widely used for fabricating 2-D quantum well nanostructures (Gruber *et al.*, 2004; Makino *et al.*, 2005; Bakin *et al.*, 2007; Lawrie *et al.*, 2012). The researchers (Gruber *et al.*, 2004; Bakin *et al.*, 2007; Lawrie *et al.*, 2012) modified the properties of $Zn_{1-x}Mg_xO$ by controlling the magnesium content *(x)* to optimize the carrier confinement in the quantum well. Lawire *et al*. (Lawrie *et al.*, 2012) have reported the strong plasmonic interaction in ZnO/ $Zn_{1-x}Mg_xO$ quantum wells with $x=0.15$. The tuning of the quantum well width has been used to modify the weak-coupling into strong coupling. Gurber *et al.* (Gruber *et al.*, 2004) have modified the content of magnesium $x<0.10$ to achieve the blue shift in the photoluminescence. Bakin *et al.* (Bakin *et al.*, 2007) have reported 2-D nanostructure embedded into 1-D nanostructure. They (Bakin *et al.*, 2007) have also fabricated ZnO nanopillers with ZnO/ZnMgO quantum well embedded on it to achieve the fabrication

of nano LEDs. The major works on ZnO based quantum well nanostructure are reported for the luminescence applications. However, the synthesis of controlled $Zn_{1-x}Mg_xO$ requires complex and sophisticated facilities which increase the fabrication cost.

1.6.2 ZnO Nanowire Based UV Photodetectors

The ZnO Nanowires (NWs) based devices have been extensively studied for multiple applications such as for the fabrication of LEDs (Bakin *et al.*, 2007), field effect transistors (Farmakis *et al.*, 2008), thin film transistor (Li *et al.*, 2008), water splitting (Dotan *et al.*, 2013), piezoelectricity (Periasamy and Chakrabarti, 2011), bio sensing (Wei *et al.*, 2006), and UV photodetectors (Basak *et al.*, 2003; Liu *et al.*, 2007; Soci *et al.*, 2007; Das *et al.*, 2010; Bai *et al.*, 2011). The UV sensing in ZnO NWs has been reported back in 2002 by Kind *et al.* (Kind *et al.*, 2002). They (Kind *et al.*, 2002) have synthesised ZnO NWs with the diameter ranging from ~50 nm to 300 nm using vapour phase transport method. The patterned Au contacts are fabricated on the ZnO NWs using electron beam lithography (Kind *et al.*, 2002). The UV illumination is used to vary the conductivity of the nanowires to make the device as an optical switch (Kind *et al.*, 2002). Cheng et al. (Cheng *et al.*, 2011) have reported Au/ZnO NWs based Schottky UV photodetectors using thermal evaporation technique. They (Cheng *et al.*, 2011) have achieved responsivity of 2.6 x 10^3 A/W. An ZnO NWs based metal-semiconductor-metal (MSM) UV photodetector has been reported by Guo et al. (Guo *et al.*, 2012). They (Guo *et al.*, 2012) have fabricated an interdigitated Au MSM electrode structure (with finger spacing 6.5μm) by sputtering method on the ZnO NWs by synthesized by the dielectrophoresis method. They (Guo *et al.*, 2012) have measured the responsivity of 40 A/W under UV illumination. The ZnO NWs based UV photodetectors are reported with various device structures (Liu *et al.*, 2010).

1.6.3 ZnO Quantum Dots/Nanoparticles Based UV Photodetectors

The colloidal QDs possess various attractive properties such as the band gap tuning by modifying the particle size during the synthesis, and controllable charge transport and trap states by modifying the surface properties using a suitable surface passivation ligands (Murphy, 2002). The QDs have much larger surface to volume ratio over their bulk counterparts which make them suitable for photodetection (Kumar, Kumar, Mukherjee, *et al.*, 2017), solar cell (Yuan *et al.*, 2016), and bio-sensing (Kumar *et al.*, 2014) applications. CQDs of several materials such as the CdSe (Oertel *et al.*, 2005), PbS (Pal *et al.*, 2012), PbSe (Wang *et al.*, 2015), ZnO (D.-Y. Guo *et al.*, 2014), (Xu *et al.*, 2014) and HgTe (Keuleyan *et al.*, 2011) can be used for photodetection applications. Among them, ZnO CQDs are the promising materials for fabricating UV photodetectors. Although ZnO QDs based devices can be fabricated by using almost all the physical and chemical deposition methods, however, the solution processing based synthesis of ZnO QDs may be considered as the simplest and most cost effective method for fabricating the large area nanoelectronic devices (D.-Y. Guo *et al.*, 2014; Xu *et al.*, 2014). Jin *et. al* (Jin *et al.*, 2008) have reported a visible-blind ZnO Nanoparticles (NPs) based UV photodetector on a low-cost glass substrate. They (Jin *et al.*, 2008) have achieved a responsivity of 61 A/W under the high UV illumination intensity of 1.06 mW/cm^2. ZnO NPs along with a suitable metal such as Au have been used to enhance the multifunctions of the ZnO NPs by inducing plasmonic effects (Gogurla *et al.*, 2014). They (Gogurla *et al.*, 2014) used Au-ZnO nanoparticles for UV detection and nitrogen oxide detection at room temperature. The Au-ZnO nanoparticles have been reported to enhance the photoresponse by about 80 times as compared to only ZnO NPs based devices. The charge transfer mechanism in QDs performed via tunnelling and

hoping can be approximated using Marcus theory (Klimov, 2010). The existence of small back to back Schottky barrier between the adjacent QDs is reported to reduce the flow of charge carriers between the electrodes (Xu *et al.*, 2014) in ZnO QDs based devices. Guo *et. al* (D.-Y. Guo *et al.*, 2014) have fabricated carbon doped ZnO QDs to improve the charge transportation between the QDs and achieved a high detectivity of 3.1×10^{17} $cmHz^{1/2}/W$. Optical properties of the ZnO QDs are reported to be tuned by changing the particle size of the ZnO QDs due to the change in the band gap of the QDs (Lin *et al.*, 2006). They (Lin *et al.*, 2006) have observed the blue shift and quantum confinement in ZnO QDs due to the band gap change owing to the variation in the size of the ZnO QDs. The band gap tuning property and the discrete energy bands of the ZnO QDs can be explored for designing the spectrum selective UV photodetectors.

1.6.4 ZnO Based Spectrum Selective UV Photodetectors

Wide absorption spectrum of bulk ZnO due to the continuum energy states in the conduction and valence bands results in a poor sensitivity and hence is not suitable for the high quality spectrum selective UV photodetectors. In order to achieve high spectrum selectivity, Zhu et al. (Zhu *et al.*, 2008) have fabricated an n-ZnO/p-GaN heterojunction UV photodetector by depositing an undoped ZnO film onto a commercially available GaN/Al_2O_3 substrate using plasma-assisted molecular beam epitaxy (MBE) technique. The p-GaN on the ZnO film is used to act as a "filter" to enhance the spectrum selectivity by reducing the response corresponding to the low energy photons. They (Zhu *et al.*, 2008) have observed a narrow band pass response (centred at ~360nm) with selectivity in terms of the full width half maxima (FWHM) of ~17 nm and a detectivity of $1.41x10^{8}cmHz^{1/2}/W$ at 0 V bias voltage. Zhang et al. (Zhang *et al.*, 2011) have reported a wavelength selective narrow bandwidth Mg_xZn_{1-}

$_xO$/ $Mg_yZn_{1-y}O$ (where value of *x* and *y* lies between 0 to 0.5) heterostructure based MSM UV photodetector fabricated by growing $Mg_xZn_{1-x}O$/ $Mg_yZn_{1-y}O$ heteroepitaxially on double-sided-polished a-plane sapphire by the pulse laser deposition method. While the $Mg_yZn_{1-y}O$ film has been used for the active layer of the detector, the $Mg_xZn_{1-x}O$ is used to act as an optical edge filter. They (Zhang *et al.*, 2011) have measured a FWHM of ~7nm with the maximum responsivity of 1.8A/W at about ~369 nm; They (Zhang *et al.*, 2011) have also observed that the centre of the band can be shifted over 370-325 nm by different *y* : *x* combinations. Ni et al. (Ni *et al.*, 2012) have reported an i-ZnO)/n-ZnO structure based highly spectrum selective UV photodetector fabricated by depositing ZnO film on a-plane sapphire substrate by the plasma-assisted (PLD) technique. The n-ZnO layer grown on the substrate acts as an optical filter while the i-ZnO on the n-ZnO film is fabricated to act as a multiplier. They (Ni *et al.*, 2012) have obtained a FWHM of ~9 nm at ~380nm with a responsivity of ~4.91 A/W at -5V bias voltage. In contrary to the costly and sophisticated fabrication methods used in the above discussed articles, Wang et al. (Wang *et al.*, 2010) have reported an electrodeposited ZnO nanorods based spectrum selective UV detector with a FWHM of ~26 nm centred at ~364 nm but with a very poor responsivity of 0.11 A/W at -5V bias voltage. They (Wang *et al.*, 2010) have used an electrodeposited poly-N-vinylcarbazole (PVK) layer on ZnO nanorods to act as the optical filter in their device. The major drawback in all the spectrum selective ZnO nanostructure based UV detectors discussed above is the use of an additional layer for optical filtering of the selected band which make the structure a bit complex with poor responsivity due to the filtering layer. Further, none of the above studies have reported the response time

characteristics. To the best of our knowledge, no significant works on the colloidal ZnO QDs based spectrum selective UV photodetectors have been reported in the literature.

1.6.5 Major Observations from the Literature Survey

The major observations from the literature survey can be summarised as follows:

- As compared to the widely used GaN for UV detection applications, ZnO is a better option for the UV detection due to its low synthesis cost, easy processing, environment friendly non-toxic nature and direct energy band gap of ~ 3.37 eV similar to the GaN (Muñoz *et al.*, 2001; Jin *et al.*, 2008; D. Y. Guo *et al.*, 2014).

- Among various nanostructures, QDs have a very large surface-to-volume ratio. Further, the band gap energy and hence the absorption peak of the QDs can be varied by changing their particle size (Bera *et al.*, 2010).

- The fabrication of the GaN QDs requires very expensive and sophisticated instruments such as the molecular beam epitaxy (MBE) (Weidemann *et al.*, 2009) and metalorganic vapour phase epitaxy (MOVPE) (Ramvall *et al.*, 2000). However, ZnO QDs can be easily synthesized by the extremely low-cost solution processed techniques (D. Y. Guo *et al.*, 2014), (Xu *et al.*, 2014). Further, the colloidal QDs can be deposited over a variety of substrates (Krivchenko *et al.*, 2008; D. Y. Guo *et al.*, 2014; Jin *et al.*, 2014; Alaie *et al.*, 2015) by the low-cost spin coating methods without any external constraints.

- Various ZnO nanostructures based UV photodetectors have been reported in the literatures, where most of the ZnO based UV detectors have used ZnO nanowires (Basak *et al.*, 2003; Liu *et al.*, 2007; Soci *et al.*, 2007; Das *et al.*, 2010; Bai *et al.*, 2011), and ZnO thin films (Ali and Chakrabarti, 2010; Yadav, Pandey, *et al.*, 2015). However, no significant works on the ZnO CQDs based UV detectors with a narrow spectrum selective nature have been reported in the literature.

- Spectrum selectivity can be achieved from the wide spectrum based photodetectors by using external filters (Zhu *et al.*, 2008; Zhang *et al.*, 2011; Ni *et al.*, 2012; Qin *et al.*, 2013; Li *et al.*, 2015). Clearly, the use of external filtering increases the fabrication cost and reduces the photoresponse of the detectors. Further, the external filters enhance the crosstalk between the detectors (Guttosch, 2005).

1.7 Motivation and Problem Definition

ZnO is a low-cost, and direct wide band gap (~3.37 eV) semiconductor with absorption peak lying in the UV region. Further, ZnO has high thermal and chemical stabilities with high radiation hardness feature. The synthesis of colloidal ZnO QDs is a low-cost and low-temperature process. Further, the band gap tuning feature of the QDs by varying their particle size (Murphy, 2002) can be used for tuning the absorption band of the colloidal QDs (CQDs) at the desired location in the UV region of the electromagnetic spectrum. Moreover, the charge transport and trap properties of the ZnO CQDs are also controllable by involving the shell or intermediate shell in between the QDs (Chen *et al.*, 2014). The above properties of colloidal ZnO QDs are believed to

be well explored for fabricating the low-cost large-area UV photodetectors with a narrow FWHM (Full Width Half Maxima) which can be tuned by varying the size of the QDs. A thin layer of ZnO CQDs can be used as the active layer in the photoconductor and Schottky contact based UV photodetectors. The effect of colloidal ZnO NPs based scattering layer on the spectrum selectivity, responsivity and response time of a ZnO CQDs based photodetector can be also investigated.

1.8 Scopes of the Present Thesis

The basic objective of present thesis is to investigate the spectrum selectivity and responsivity of some low-cost solution processed ZnO CQDs based UV photodetectors fabricated on low-cost substrates like glass and Si substrates. The present thesis consists of Five Chapters including the present chapter. The contents of remaining four chapters are given as follows:

Chapter 2 discusses the synthesis of ZnO CQDs using hot-injection method and their characterization by using transmission electron microscopy (TEM), X-ray diffraction (XRD), and Energy dispersive X-ray spectroscopy (EDS). The thin film of ZnO CQDs was deposited over the n-Si (111) substrates using low-cost spin coating technique. The Schottky contact gold (Au) electrodes are deposited using thermal evaporation over the ZnO QDs thin films. The spectral response of the photodiode has been analyzed for the wavelengths ranging from 250 nm to 800 nm. Various electrical parameters such as the rectification ratio, ideality factor and barrier height of the Schottky photodiode under study have determined of the measured I-V characteristics. The transient response of the Au/ZnO CQDs Schottky diode based UV photodetector is studied.

Chapter 3 reports a MSM structure based interdigitated UV photodetector using ZnO CQDs as the active layer in the device. The device is fabricated on the low-cost glass substrates without using any additional absorption tuning layer. The blue shift in the band gap of ZnO QDs is analysed by changing the particle size of the QDs through annealing at two different temperatures of 450 ^{o}C and 600 ^{o}C under the ambient environment. The I-V characteristics under dark and UV illuminations have been measured. The photoresponsivity versus wavelength characteristics have been measured for 250 nm to 600 nm wavelengths. The response time and recovery time have been determined by applying UV pulses on the devices.

Chapter 4 investigates the effect of a ZnO nanoparticles (NPs) based filter cum scattering layer on the photoresponsivity and spectrum selectivity of the ZnO CQD based UV photodetector discussed in chapter 3. A layer of solution processed ZnO NPs is deposited over the colloidal quantum dots (CQDs) based Ag/ZnO CQDs/Ag interdigitated MSM photodetectors considered in Chapter-3. The photoresponse characteristics of the fabricated device is investigated under both the front and back illuminations of the UV light. The effect of the ZnO NPs on the spectrum selectivity and reponsivity of the MSM photodiode of chapter-3 has been studied in details for the back as well as front illuminated devices. Finally, the time response characteristics of the detector with ZnO NP layer have been analyzed.

Finally **Chapter 5** has been devoted to summarise the major findings of the thesis. At the end, the future scopes of works related to the present thesis have been briefly outlined.